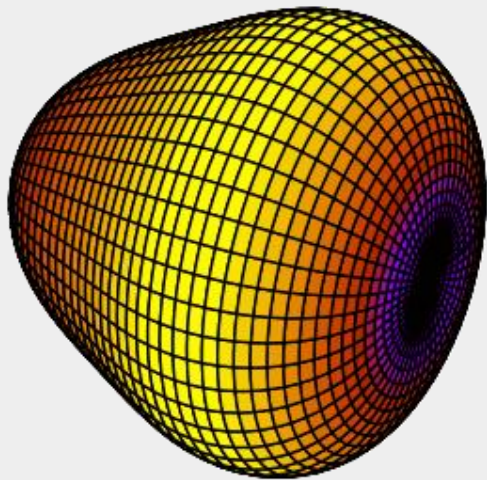


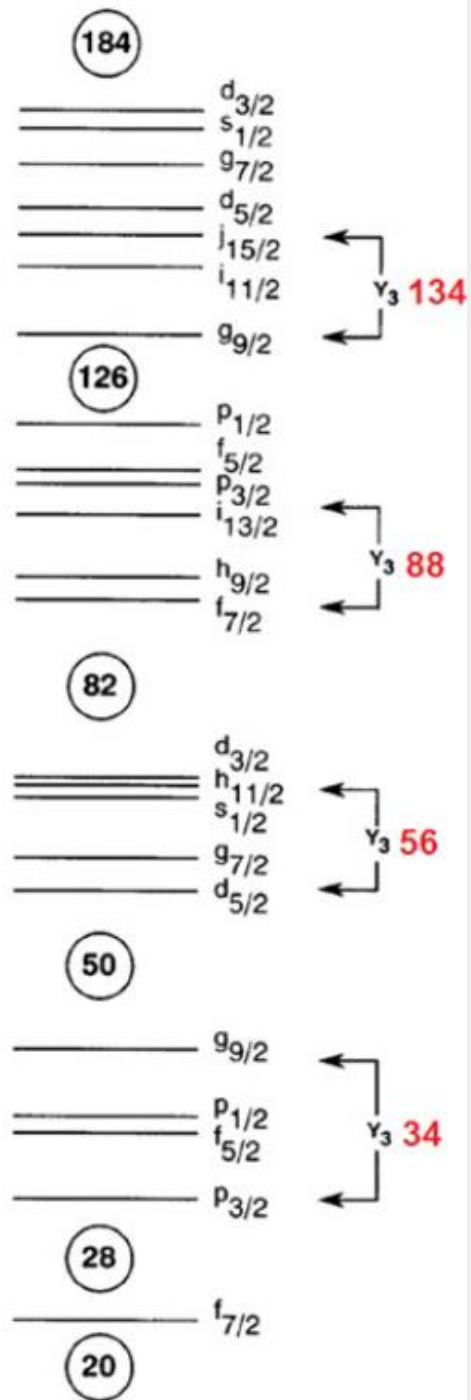
# Measurements of octupole collectivity in $^{144}\text{Ba}$



Ben Jones  
University of Liverpool

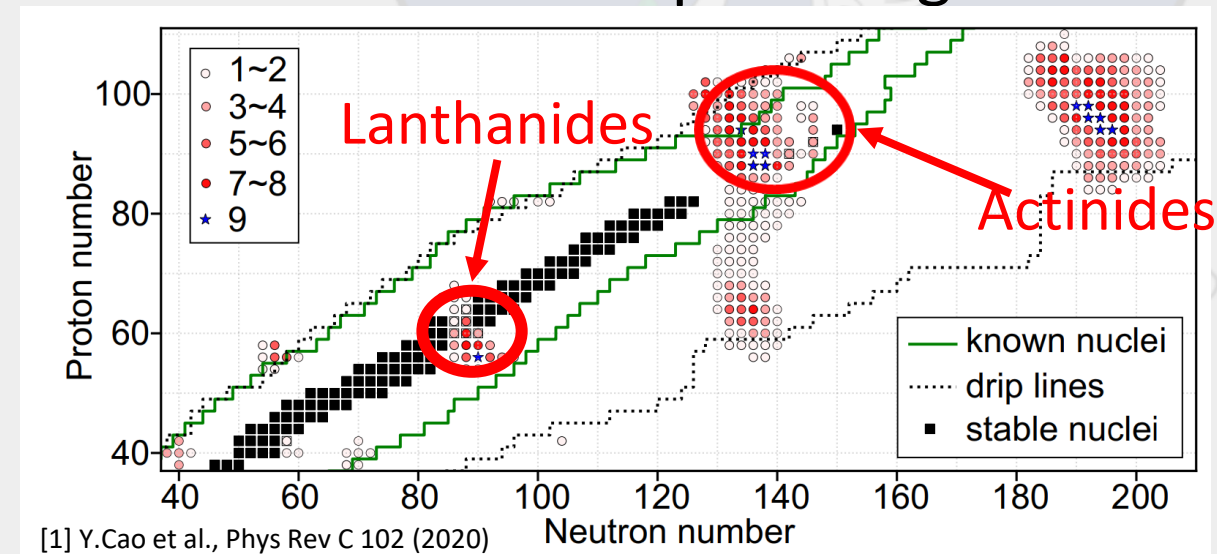


Intruder orbitals



# Origins of octupole correlations in nuclei

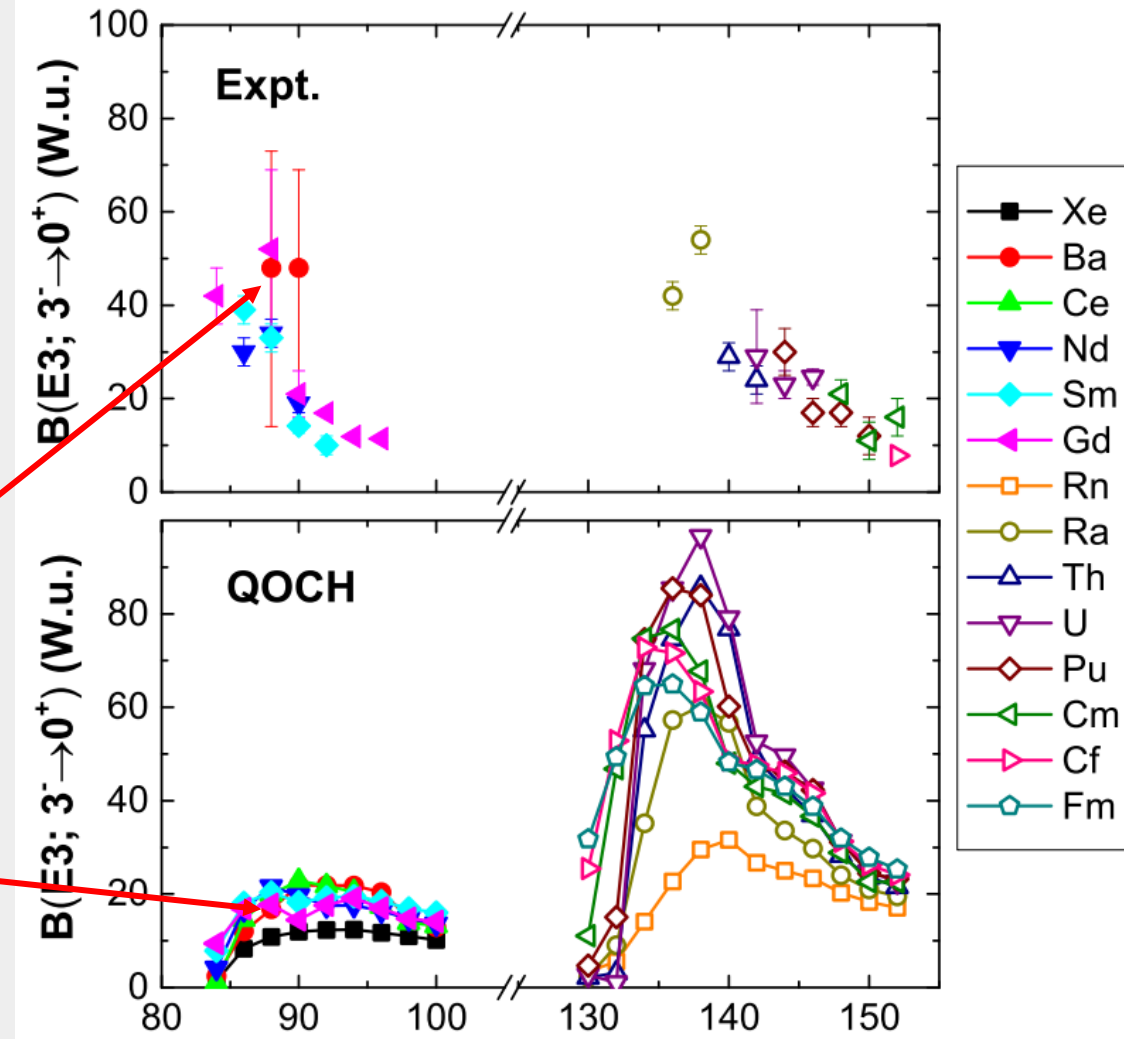
- Octupole deformations can be traced back to particle-hole interactions with intruder orbitals of opposite parity with  $\Delta j, \Delta l = 3$ , coupled by the octupole interaction.
- Octupole magic numbers: 34, 56, 88, 134.
- Octupole deformation is greatest when both proton and neutron numbers are near these octupole magic numbers.



[1] Y.Cao et al., Phys Rev C 102 (2020)

# Experiment vs theory

- Several Rn isotopes are shown to behave as octupole vibrators [1], and  $^{222,224,226}\text{Ra}$  exhibit static octupole deformation in their ground state [2].
- Very little experimental data of the  $B(E3)$  exists for isotopes in the Lanthanide region.
- Previous measurement of the  $B(E3)$  for  $^{144}\text{Ba}$  near by Bucher et al., ANL [3] is significantly enhanced over theory and has a large associated uncertainty.

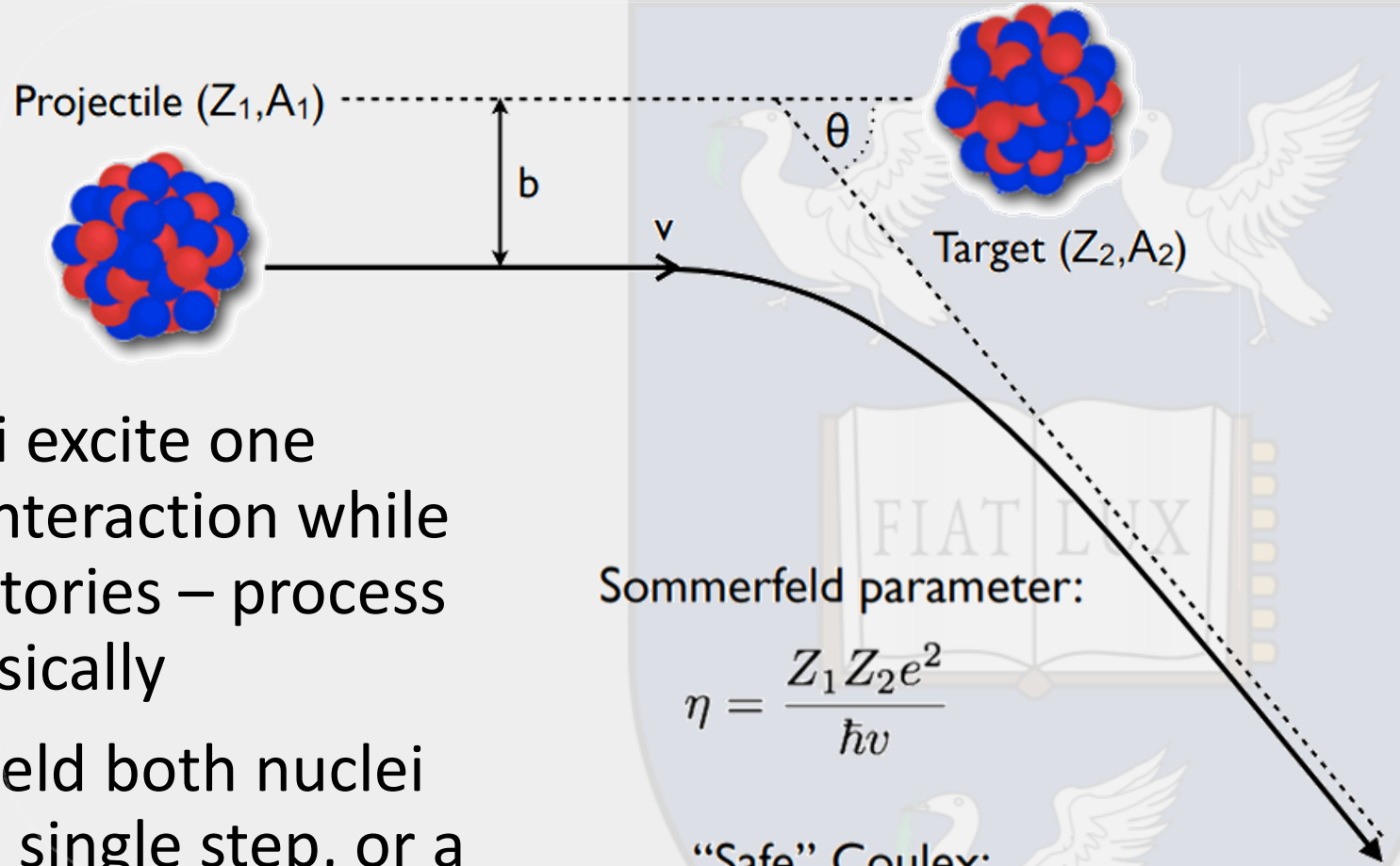


[1] P. A. Butler et al., Nat Commun. 2019 Jun 6;10(1):2473

[2] P. A. Butler et al., Phys. Rev. Lett. 124, 042503 – Published 31 January, 2020

[3] B. Bucher et al., Phys. Rev. Lett. 116, 112503 – Published 17 March, 2016

# Coulomb excitation



- Projectile and target nuclei excite one another via the Coulomb interaction while following hyperbolic trajectories – process can be modelled semi-classically
- While in each others EM-field both nuclei have a chance to excite via single step, or a series of multi-step transitions
- Direct probe for EM (E1, E2, E3, M1...) M.E.'s coupling states in a nucleus

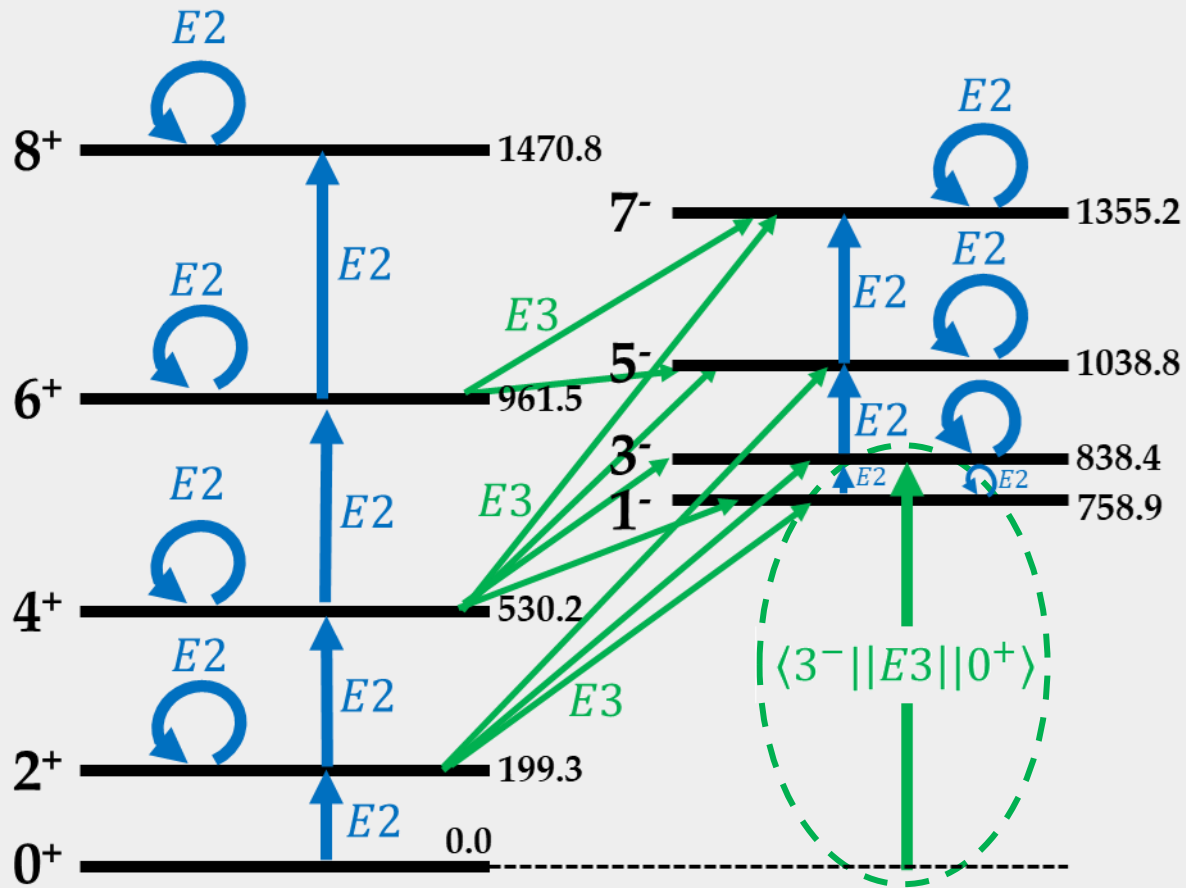
Sommerfeld parameter:

$$\eta = \frac{Z_1 Z_2 e^2}{\hbar v}$$

“Safe” Coulex:

$$\eta \gg 1$$

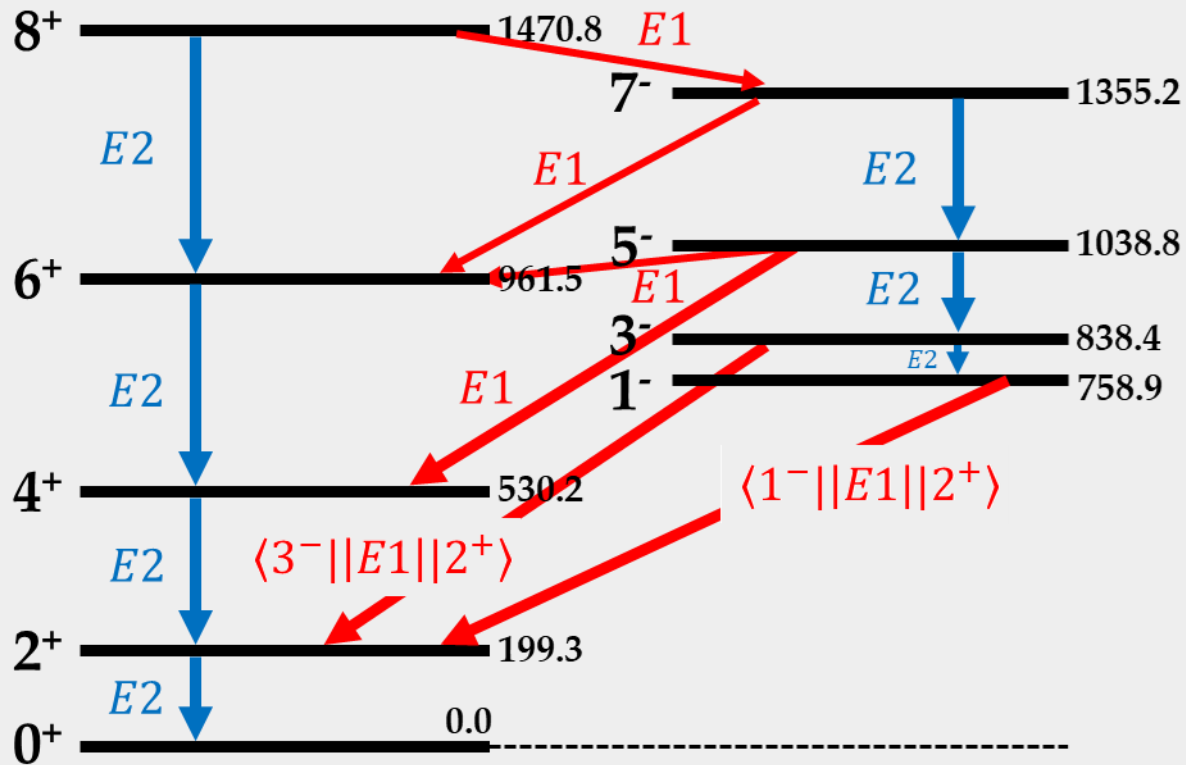
# $^{144}\text{Ba}$ – Excitation



- $E2$  and  $E3$  transitions dominate the excitation process
- Magnitude of the  $\langle 3^- || E3 || 0^+ \rangle$  M.E. is an unambiguous measure of octupole collectivity

$$B(E3; 3^- \rightarrow 0^+) = \frac{\langle 3^- || E3 || 0^+ \rangle^2}{7}$$

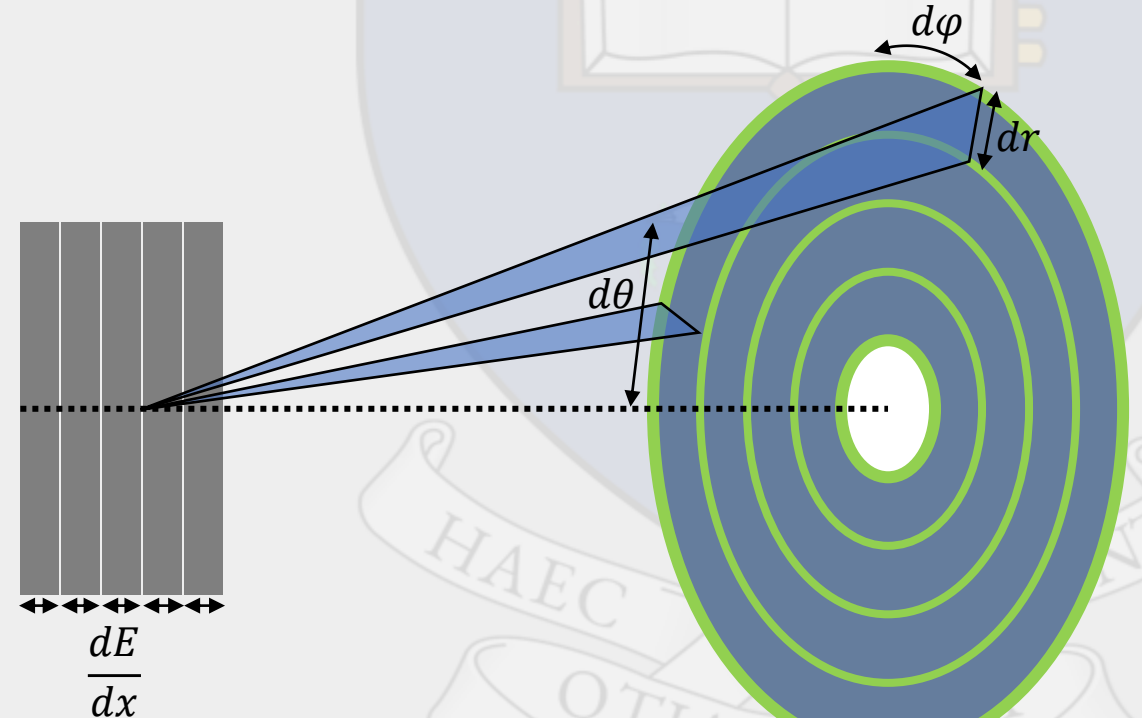
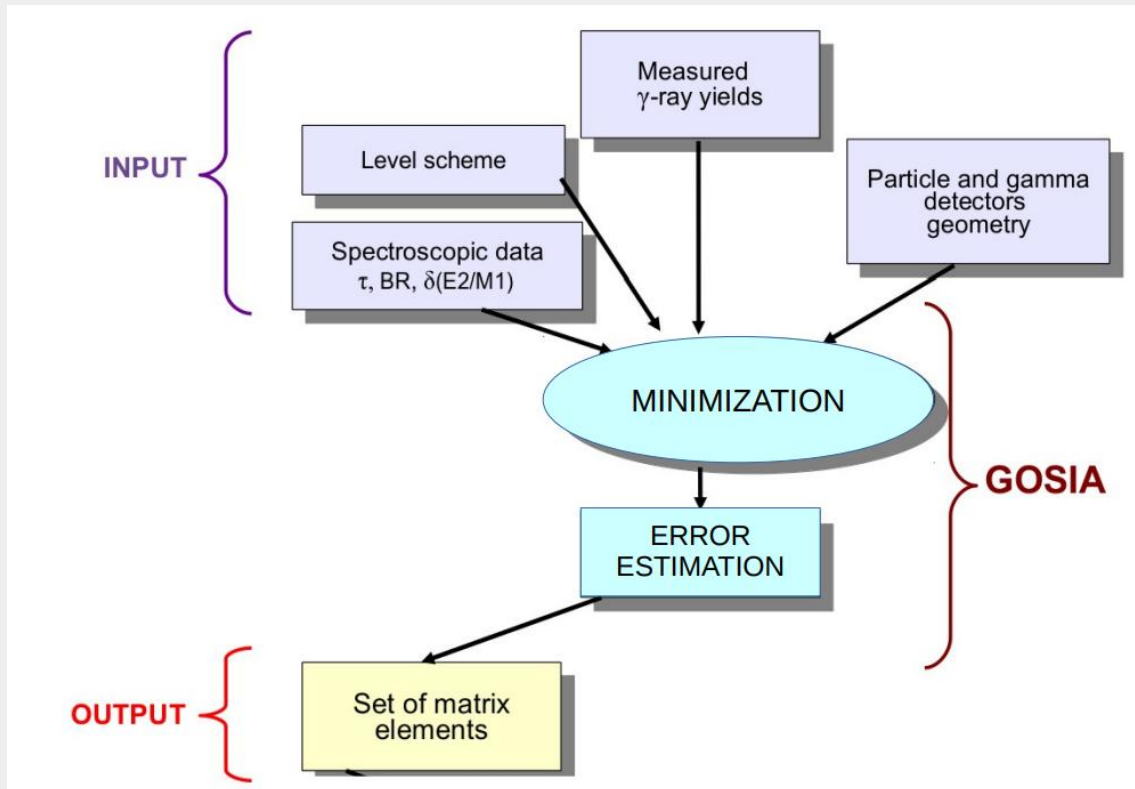
# $^{144}\text{Ba}$ – De-excitation



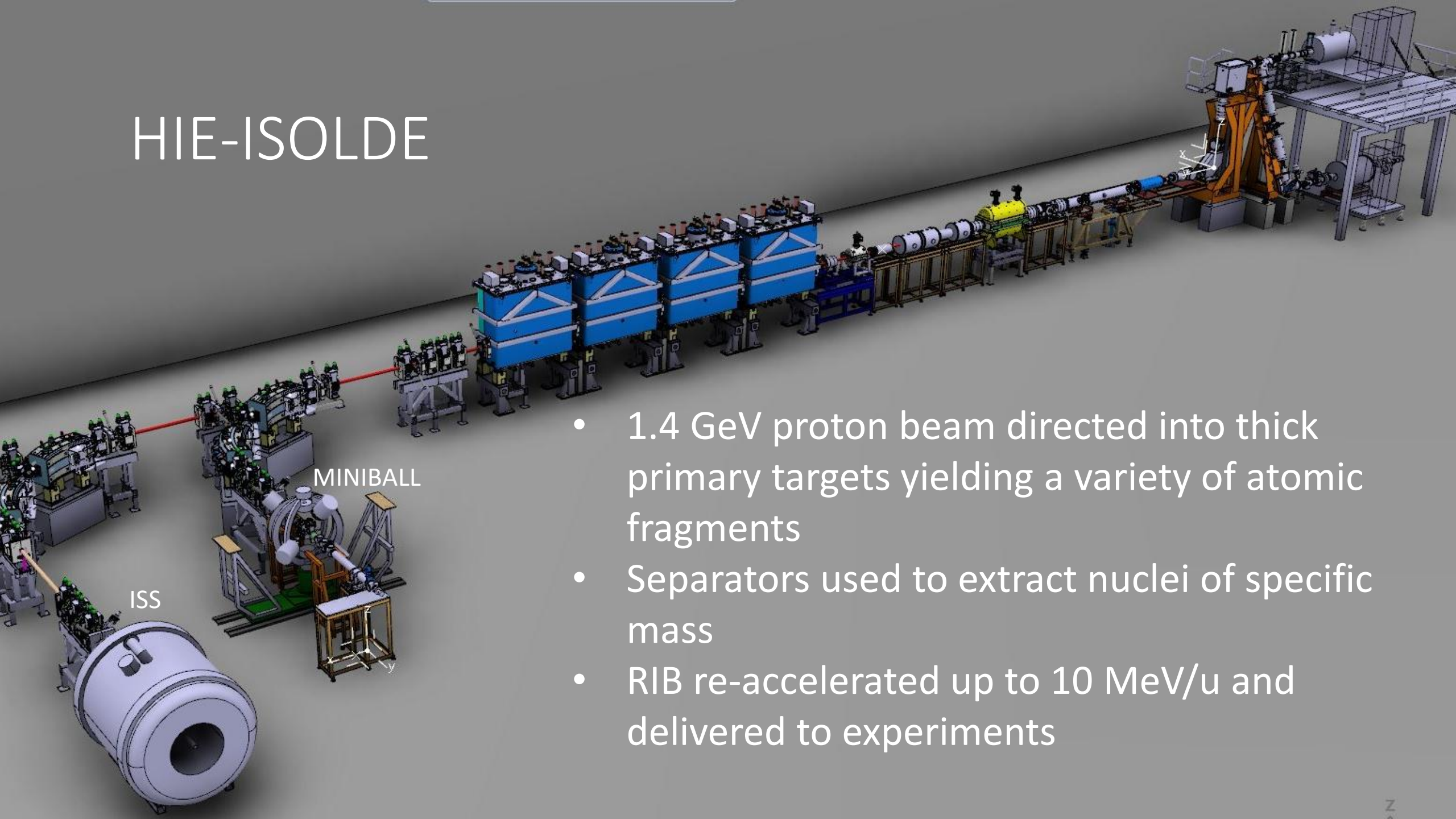
- $E2$  and  $E1$  transitions dominate the de-excitation process i.e. the observed  $\gamma$ -rays
- $3^- \rightarrow 2^+$   $\gamma$ -ray yield experimental observable used to probe occupation of the  $3^-$  state

# GOSIA

- Used to model both excitation and de-excitation process
- Integrates over target thickness and scattering angles, considering the geometry and efficiency of the detector setup
- Fits the matrix elements to the experimental particle-gated  $\gamma$ -ray yields and additional spectroscopic data



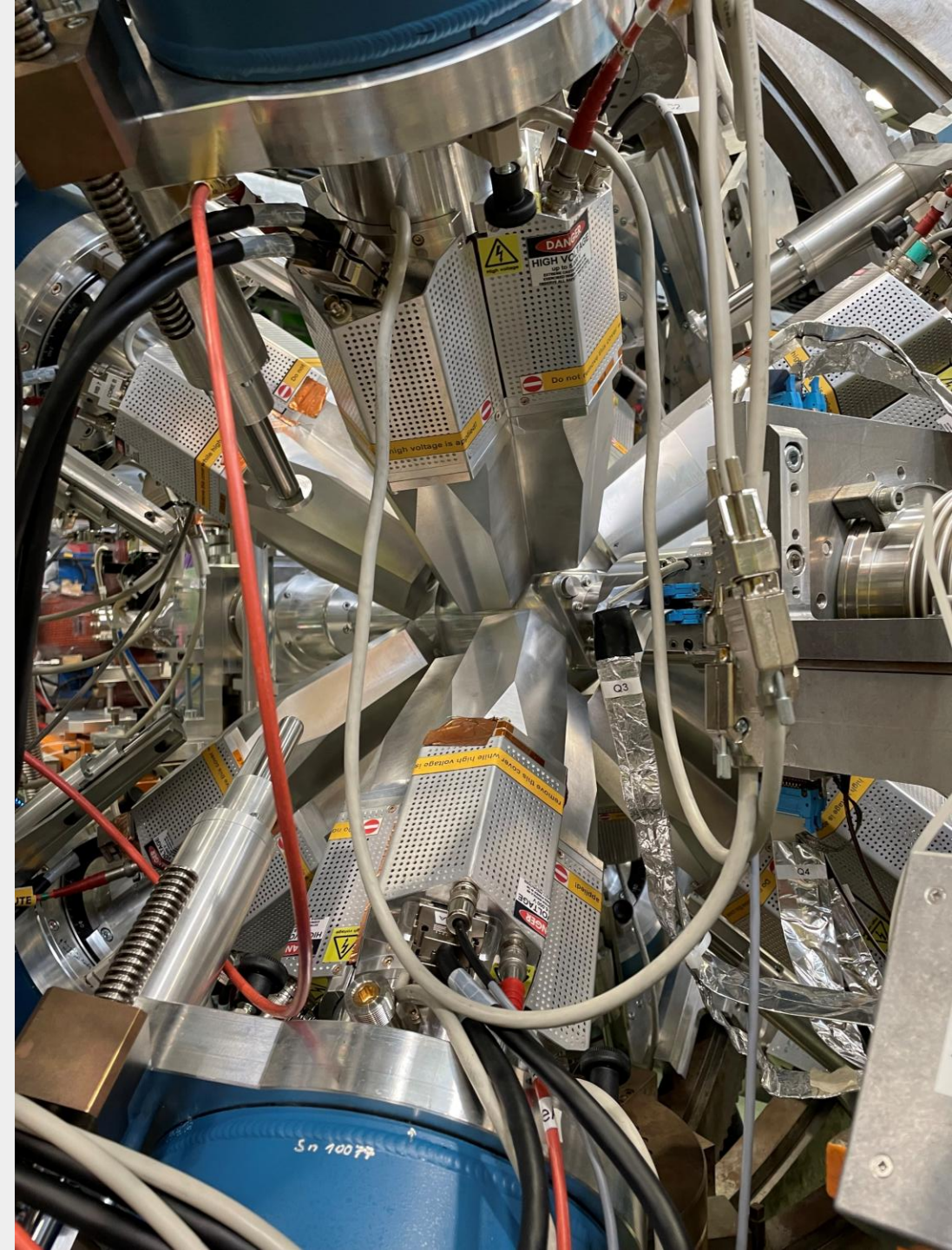
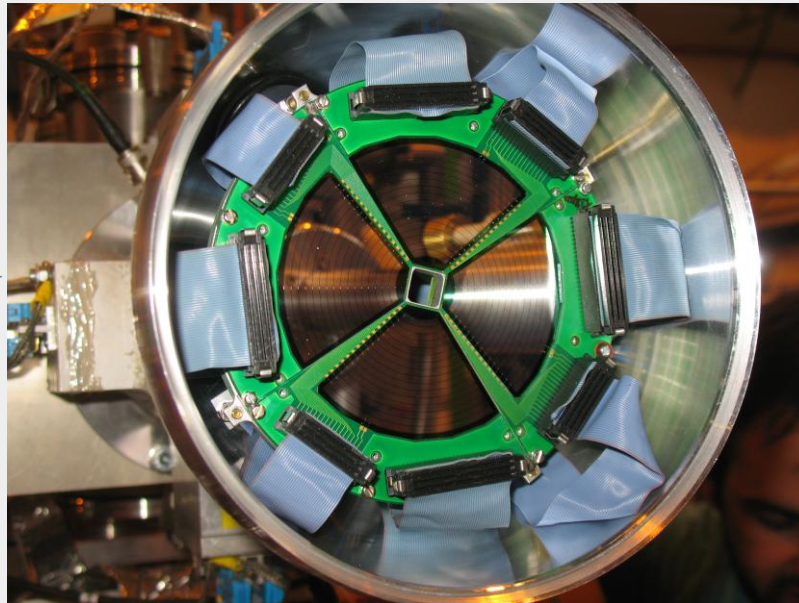
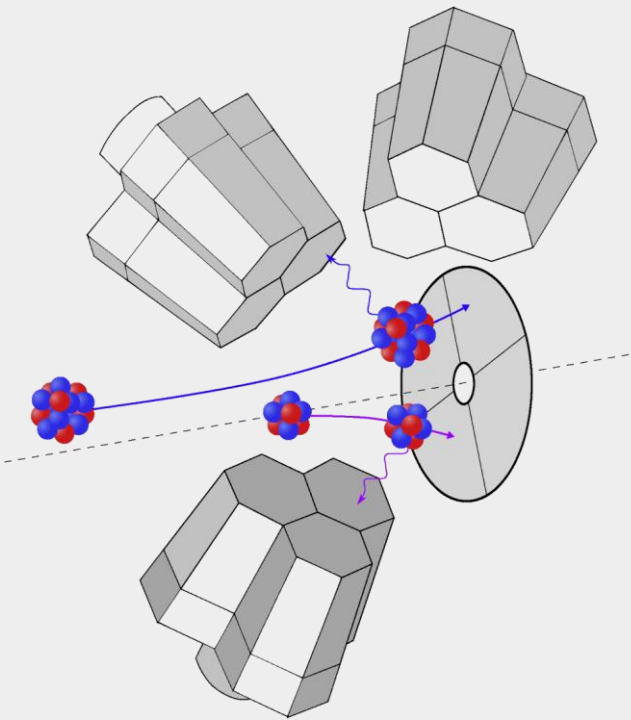
# HIE-ISOLDE



- 1.4 GeV proton beam directed into thick primary targets yielding a variety of atomic fragments
- Separators used to extract nuclei of specific mass
- RIB re-accelerated up to 10 MeV/u and delivered to experiments

# MINIBALL

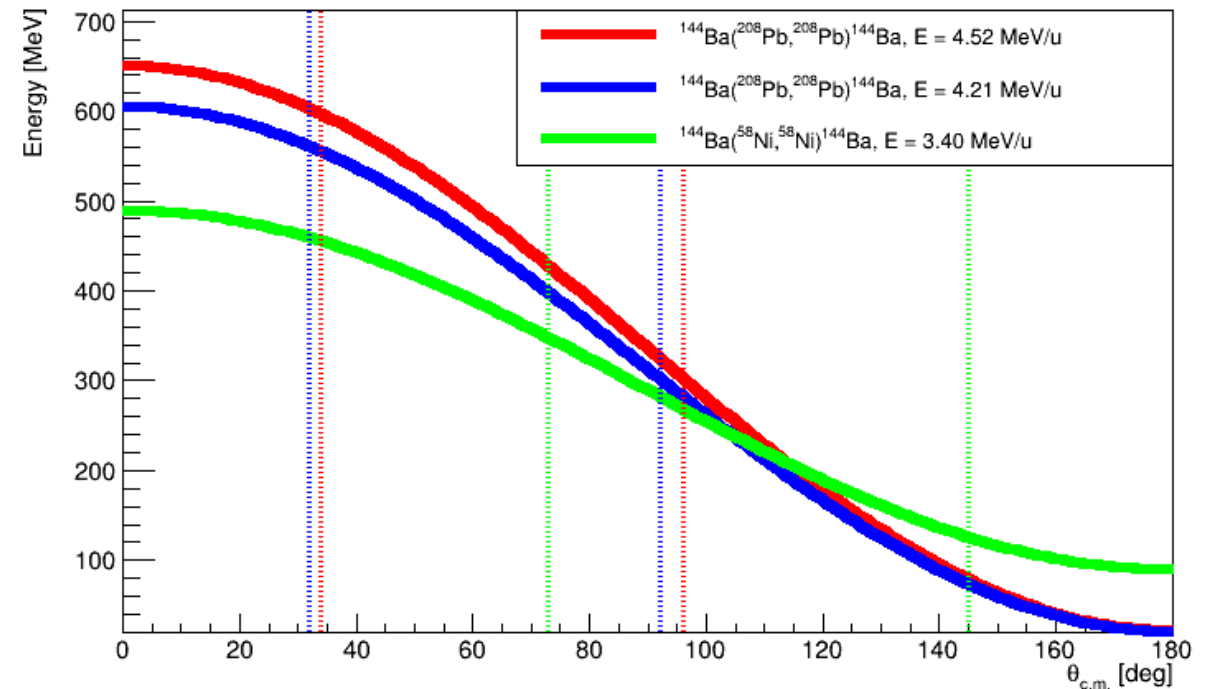
- HPGe clusters centred around the target position, plus a position sensitive silicon CD detector placed downstream of the target



# Experimental data

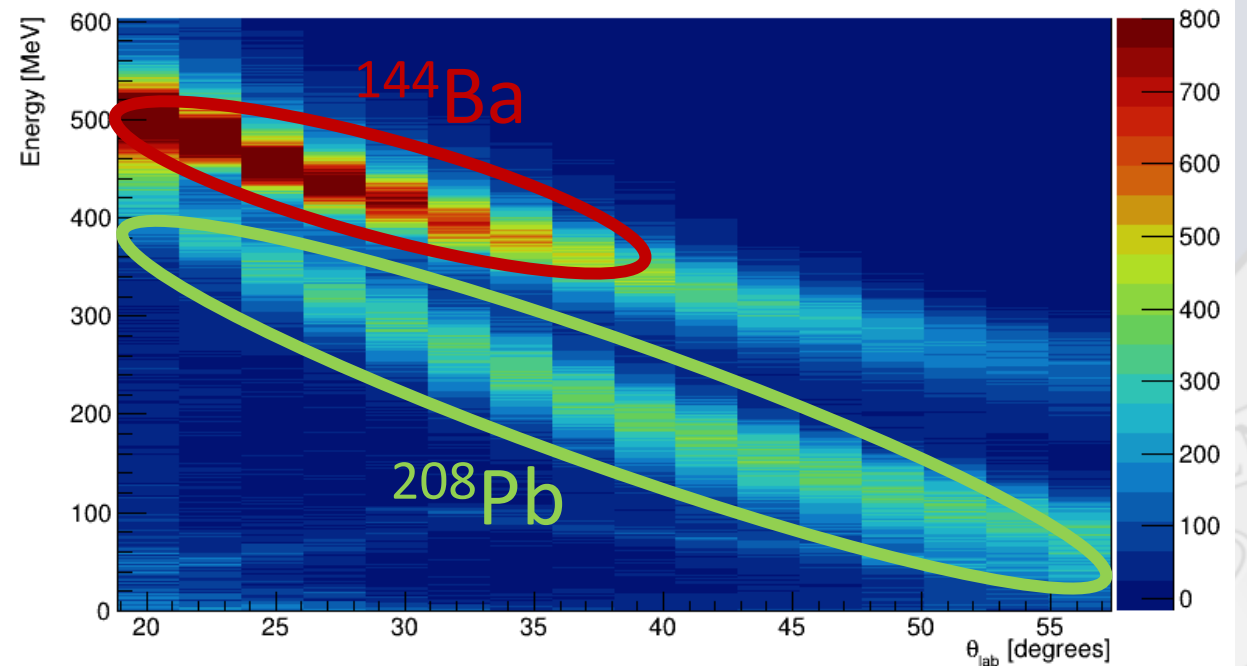
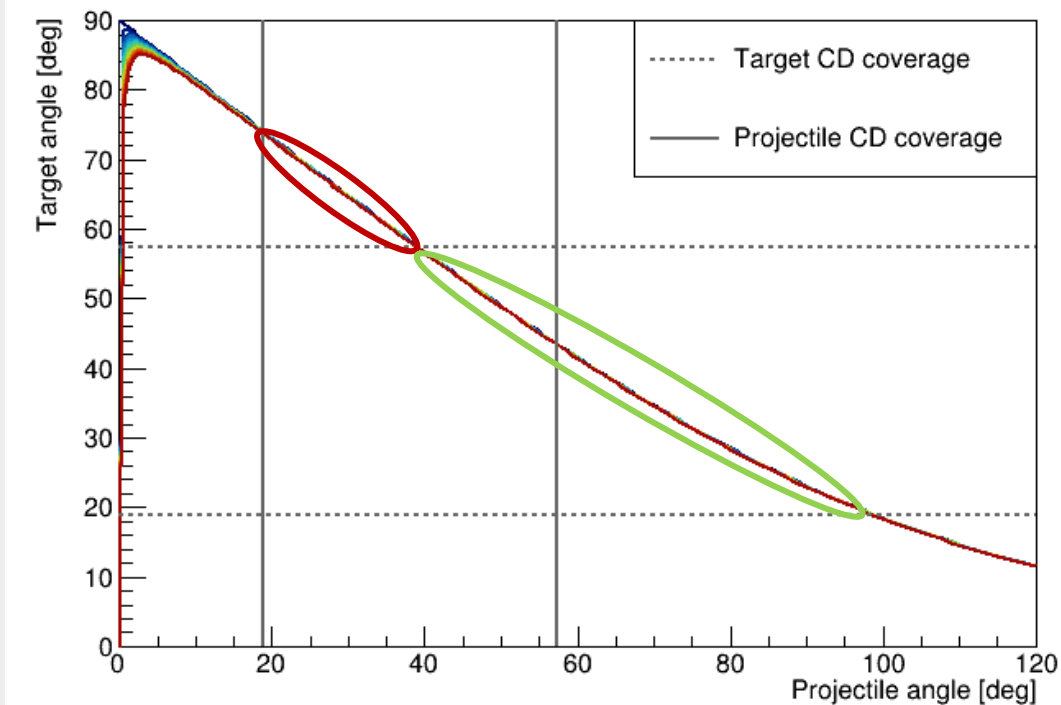
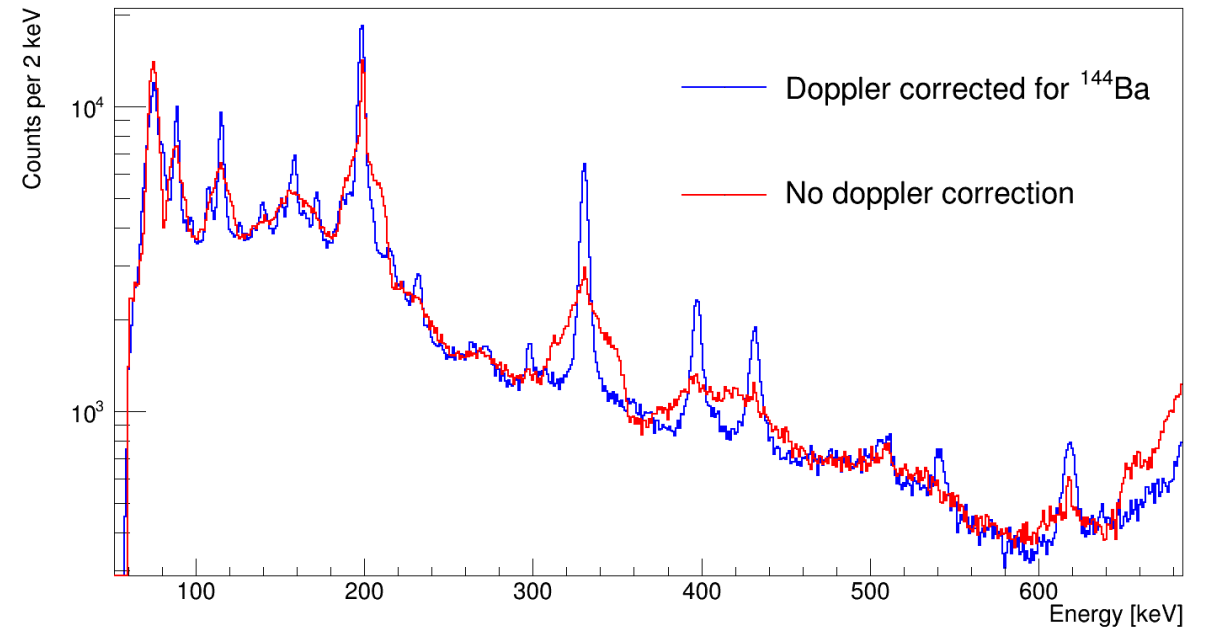
Three experiments performed on  $^{144}\text{Ba}$  over 2017 and 2024 with a mix of beam energies and target isotope to cover a greater centre-of-mass scattering angle, gaining sensitivity to the angular distributions of the excitation:

- Beam  $E = 4.21 \text{ MeV/u}$ , Target :  $^{208}\text{Pb}$
- Beam  $E = 4.52 \text{ MeV/u}$ , Target :  $^{208}\text{Pb}$
- Beam  $E = 3.40 \text{ MeV/u}$ , Target :  $^{58}\text{Ni}$



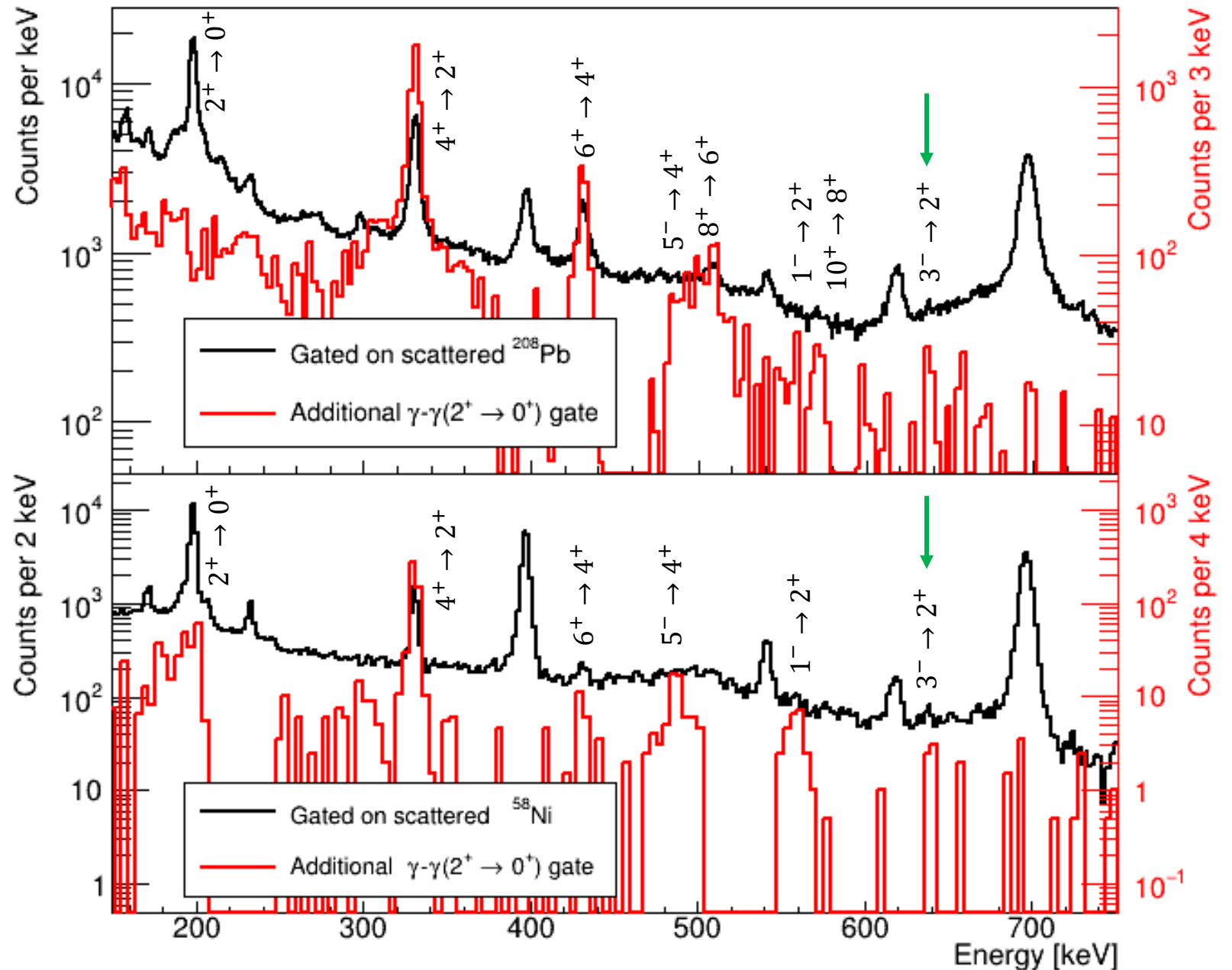
# Particle gating

- $\gamma$ -rays are doppler corrected for the coincident projectile/target nucleus
- Gating on both the projectile and target effectively increases the lab angle coverage of the CD detector



# Particle gated spectra

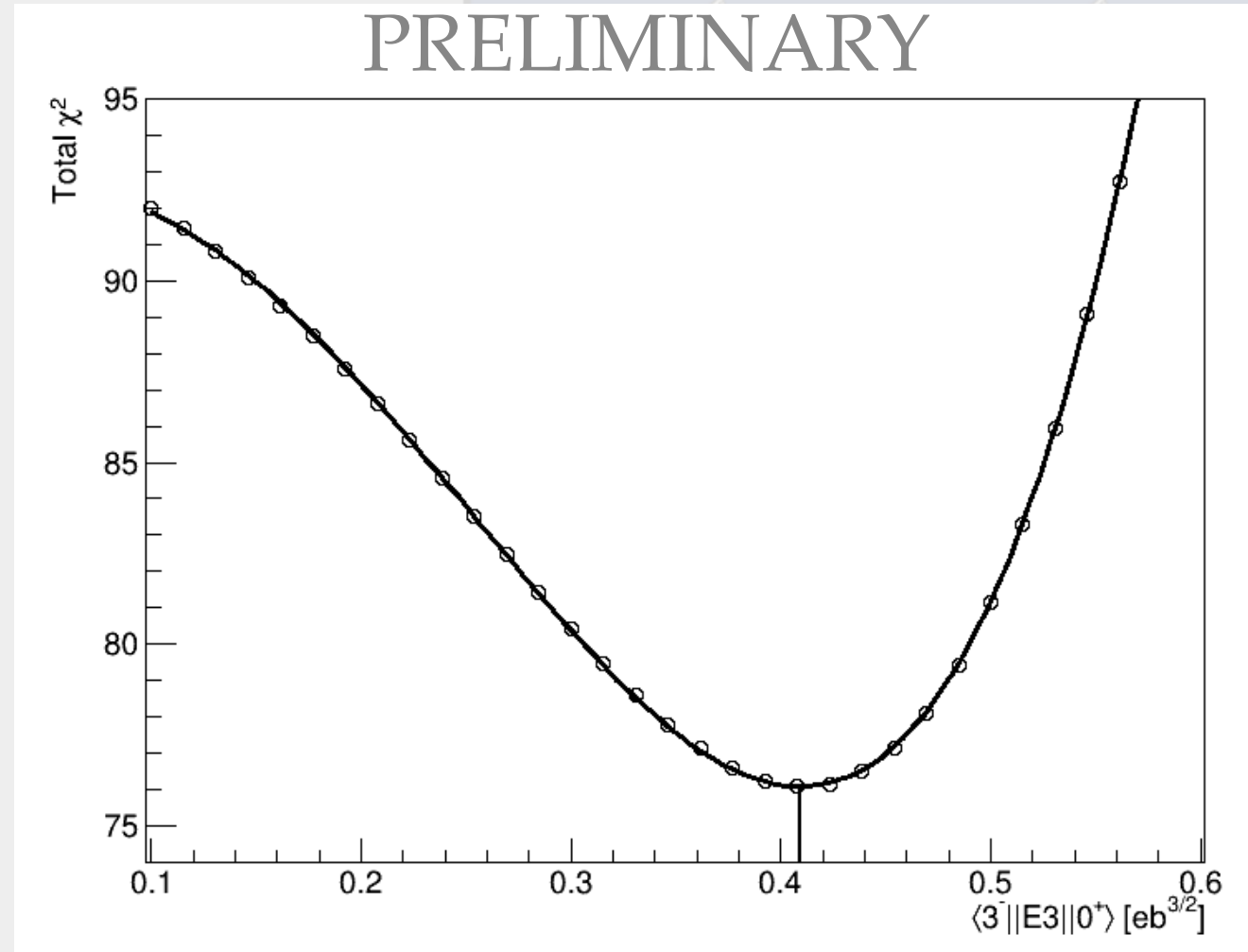
- Singles and  $\gamma$ - $\gamma$  yields checked for consistency for low yield peaks
- $^{208}\text{Pb}$  target favours multistep excitation and has higher Coulomb excitation cross section
- $^{58}\text{Ni}$  target favours single step excitation and has fewer counts, but cleaner spectrum



# GOSIA – $\chi^2$ minimisation

- Data normalised to known lifetime of the  $4^+ \rightarrow 2^+$  in  $^{144}\text{Ba}$
- $\chi^2$  scan of  $\langle 3^- || E3 || 0^+ \rangle$ , all other M.E.'s are allowed to vary during the minimisation

$$B(E3; 3^- \rightarrow 0^+) = \frac{\langle 3^- || E3 || 0^+ \rangle^2}{7}$$

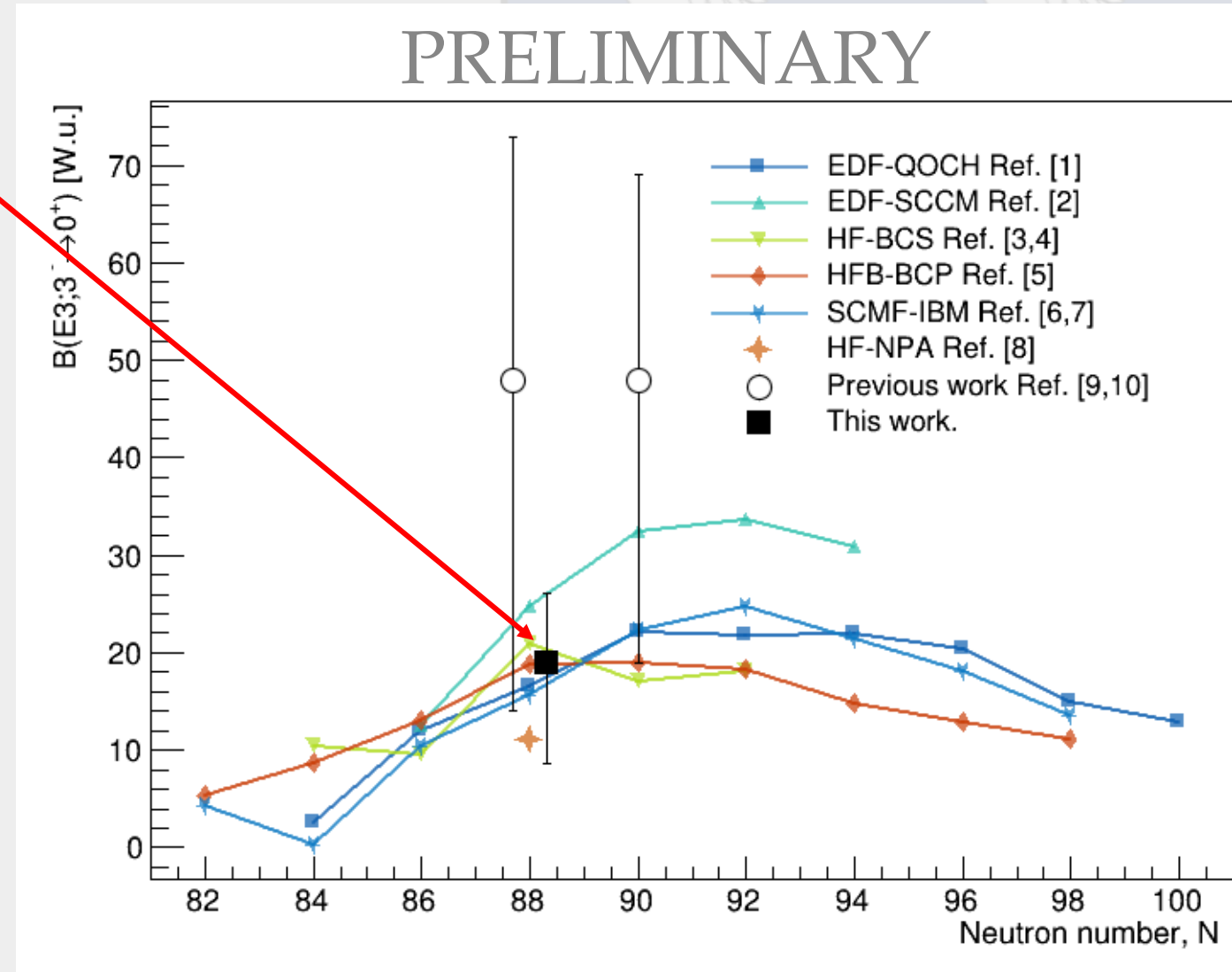


# Measured $B(E3; 3^- \rightarrow 0^+)$

- Extracted  $B(E3)$  consistent with current theory
- Systematic errors yet to be included (Beam energy, target thickness etc.)

## References:

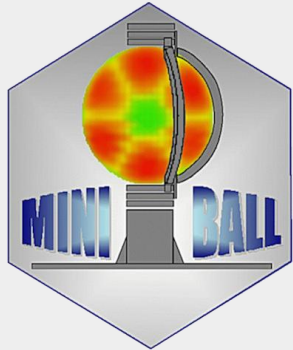
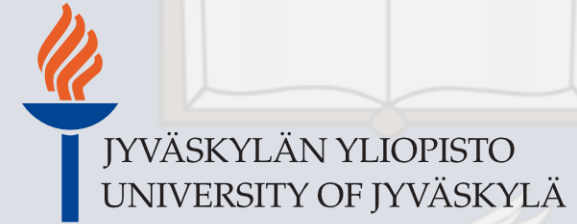
- [1] S. Y. Xia et al., Phys. Rev. C 96, 054303 (2017)
- [2] R. N. Bernard, L. M. Robledo and T. R. Rodríguez, Phys. Rev. C 93, 061302 (2016)
- [3] J. Egido and L.M. Robledo, Nucl. Phys. A 518, 475 (1990)
- [4] J. Egido and L.M. Robledo, Nucl. Phys. A 545, 589 (1992)
- [5] L. M. Robledo, M. Baldo, P Schuk, and T. R. Rodríguez, Phys. Rev. C 81, 034315 (2010)
- [6] K. Nomura, D. Vretenar, T. Nikšić and Bing-Nan Lu, Phys. Rev. C 89, 024312 (2014)
- [7] K. Nomura, T. Nikšić and D. Vretenar, Phys. Rev. C 97 024317 (2014)
- [8] X. Yin, M. Q. Lin, C. Ma, and Y. M. Zhao, Phys. Rev. C 111, 044310 (2025)
- [9] B. Bucher et al., Phys. Rev. Lett. 116. 112503 (2016)
- [10] B. Bucher et al., Phys. Rev. Lett. 118. 152504 (2017)



# Outlook

- Complementary analysis of the  $2^+ \rightarrow 0^+$  lifetime from this dataset – compare ratio of doppler shifted and unshifted  $\gamma(2^+ \rightarrow 0^+)$  yield
- GOSIA analysis of isobaric contaminants in the beam ( $^{144}\text{Sm}$  and  $^{144}\text{Nd}$ ) will provide consistency check with previous B(E2) and B(E3) measurements
- Data from  $^{144}\text{Ba}(d,d')$  measurement at ISS to extract deformation lengths,  $\beta_\gamma$ , currently being analysed will hopefully provide an independent measurement B(E3)

# Thanks for listening and thanks to all the collaborators!



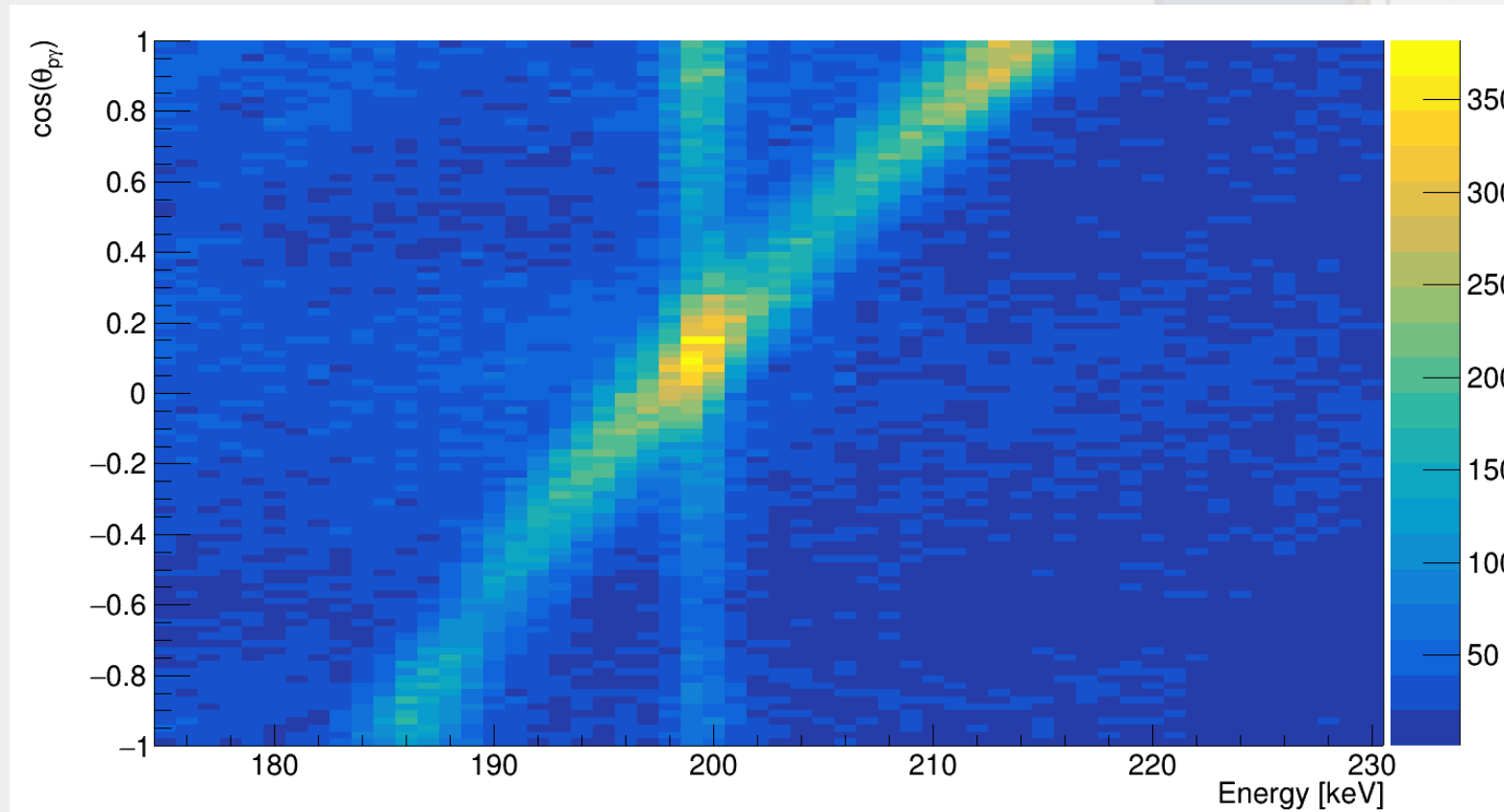
Backup slides



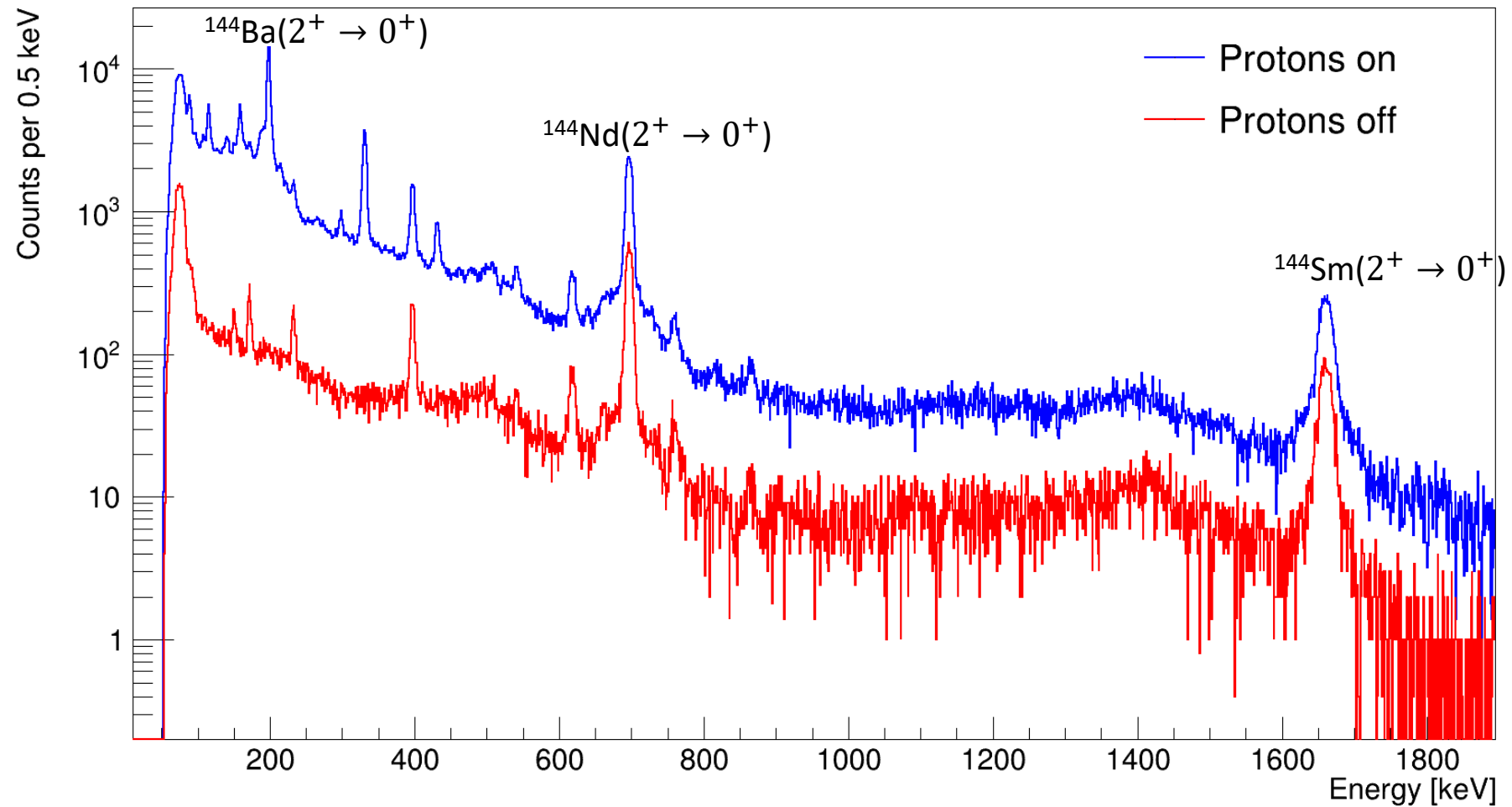
# Doppler shifted and unshifted $\gamma(2^+ \rightarrow 0^+)$

$$\lambda = \lambda_0 \frac{(1 - \beta \cos(\theta_{p\gamma}))}{\sqrt{1 - \beta^2}}$$

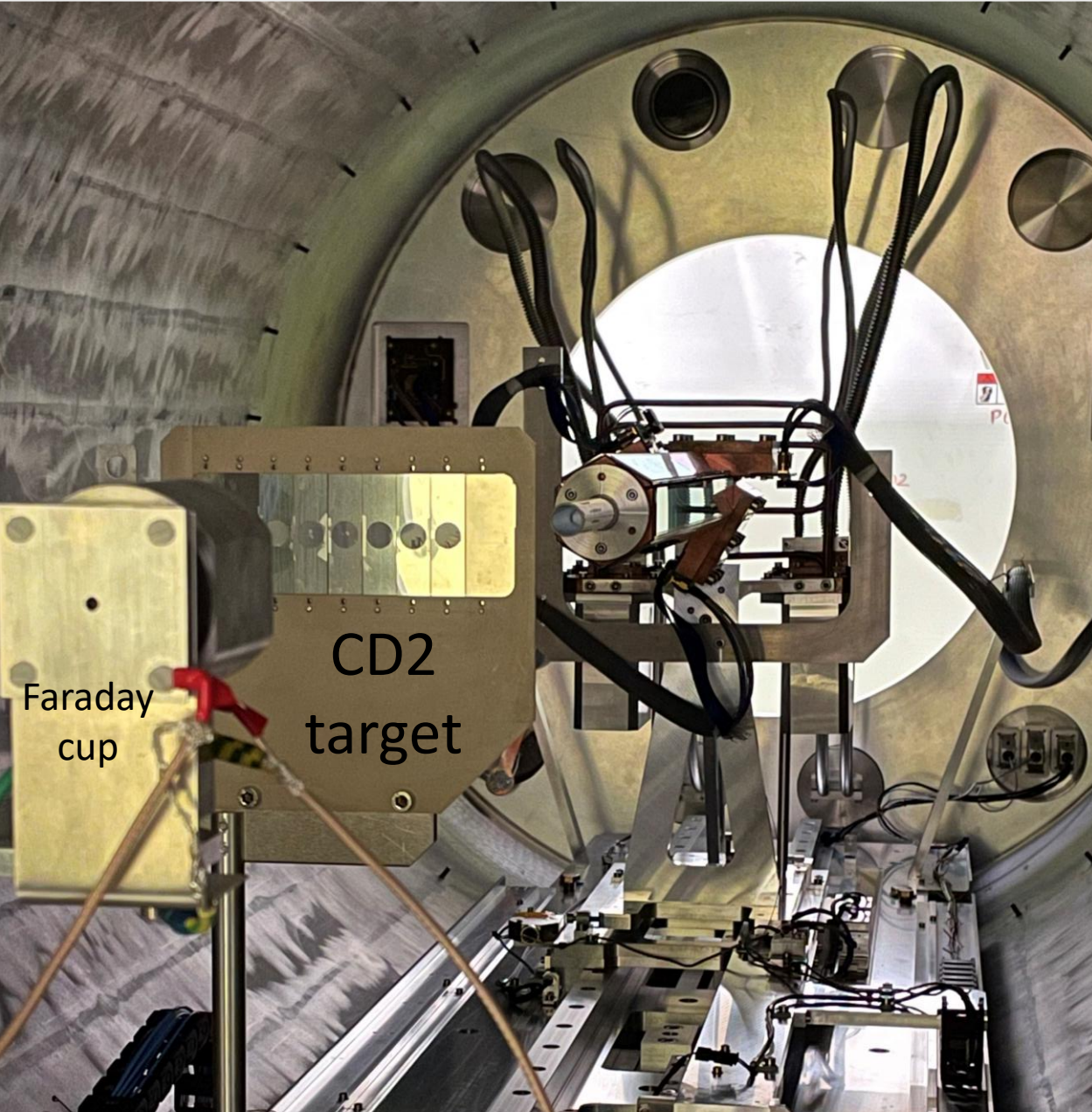
$$\frac{N(t)}{N_0} = \frac{\gamma(2^+ \rightarrow 0^+)_{shifted}}{\gamma(2^+ \rightarrow 0^+)_{shifted} + \gamma(2^+ \rightarrow 0^+)_{unshifted}} = e^{-t/\tau(2^+ \rightarrow 0^+)}$$



# Isobaric contaminants

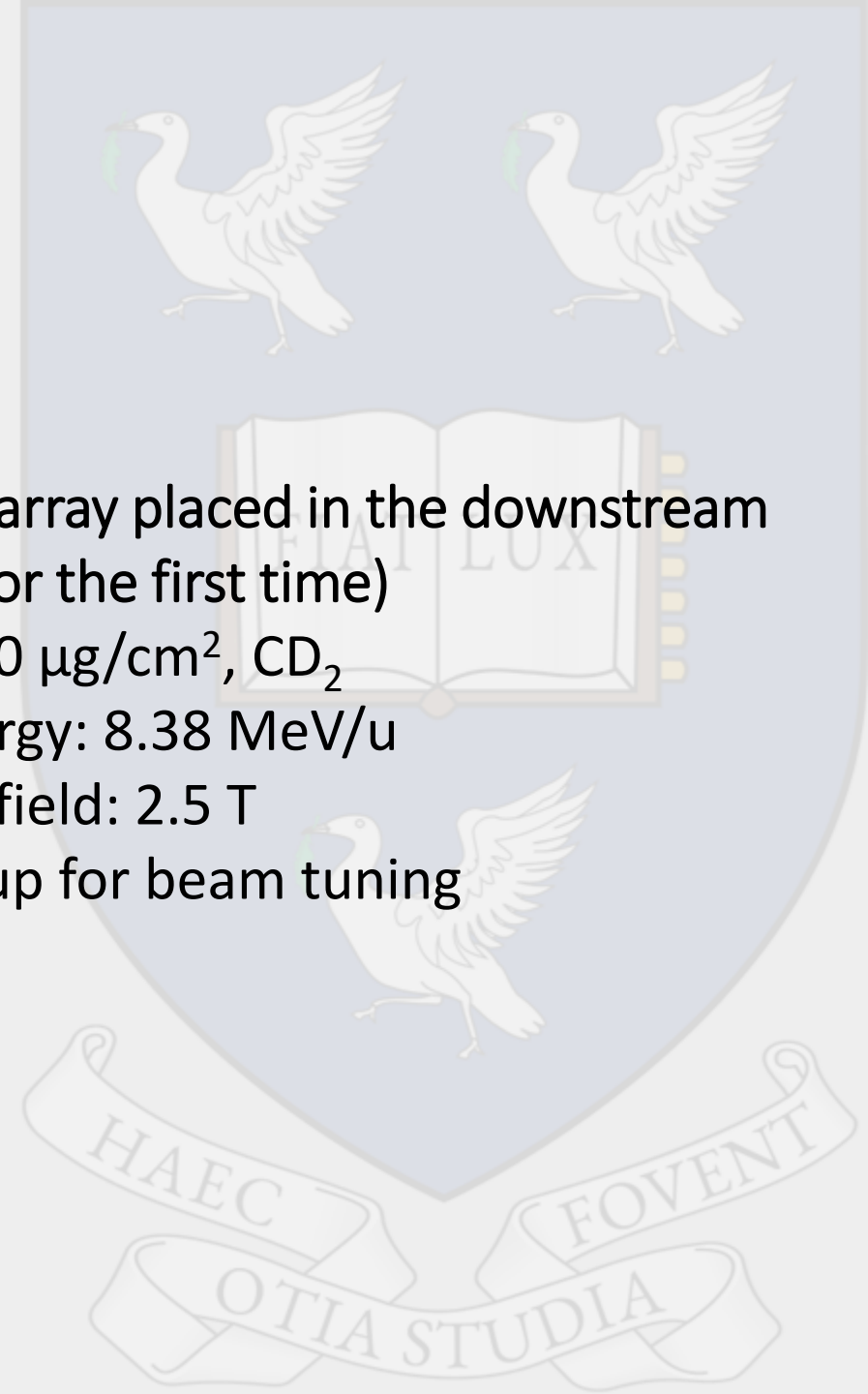


# ISS

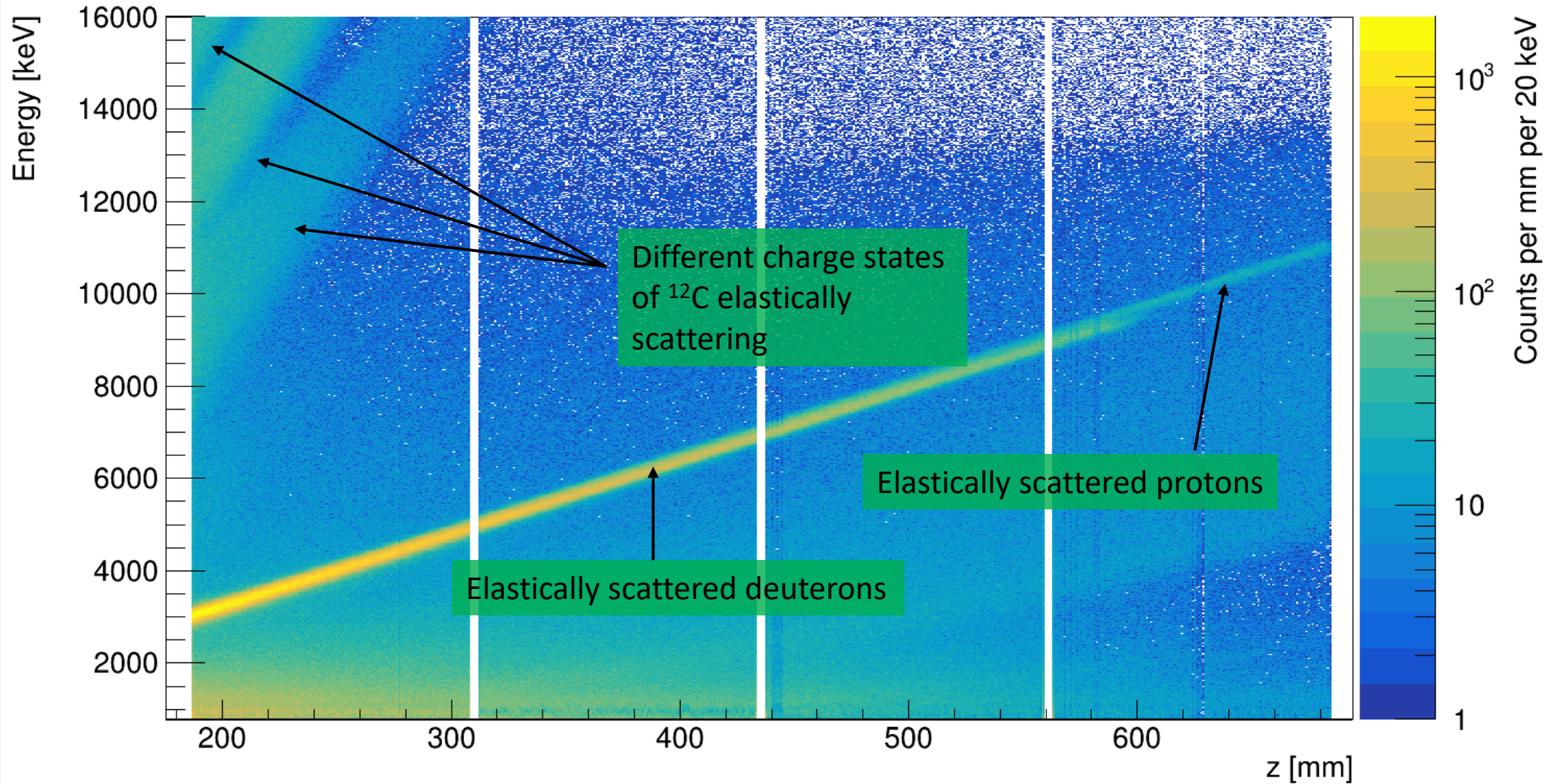


## Setup

- ISS silicon array placed in the downstream position (for the first time)
- Target:  $200 \mu\text{g}/\text{cm}^2$ ,  $\text{CD}_2$
- Beam Energy:  $8.38 \text{ MeV}/u$
- Magnetic field:  $2.5 \text{ T}$
- Faraday cup for beam tuning

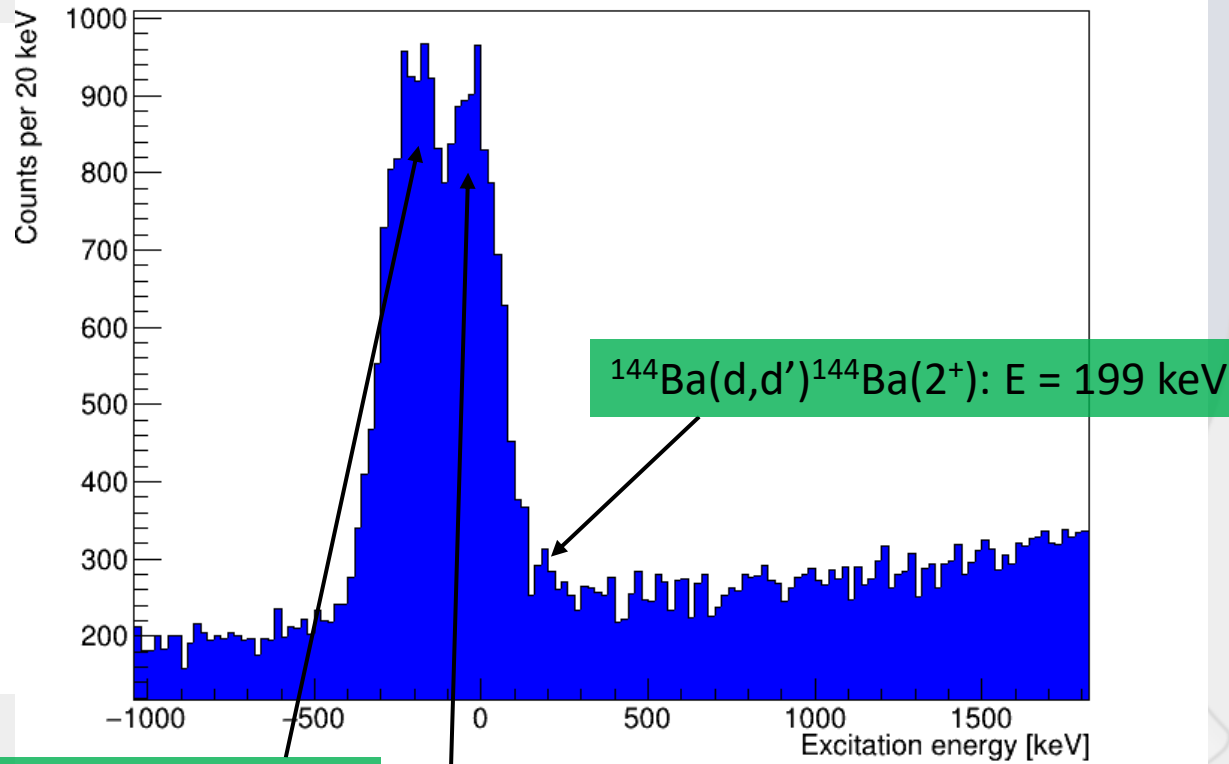
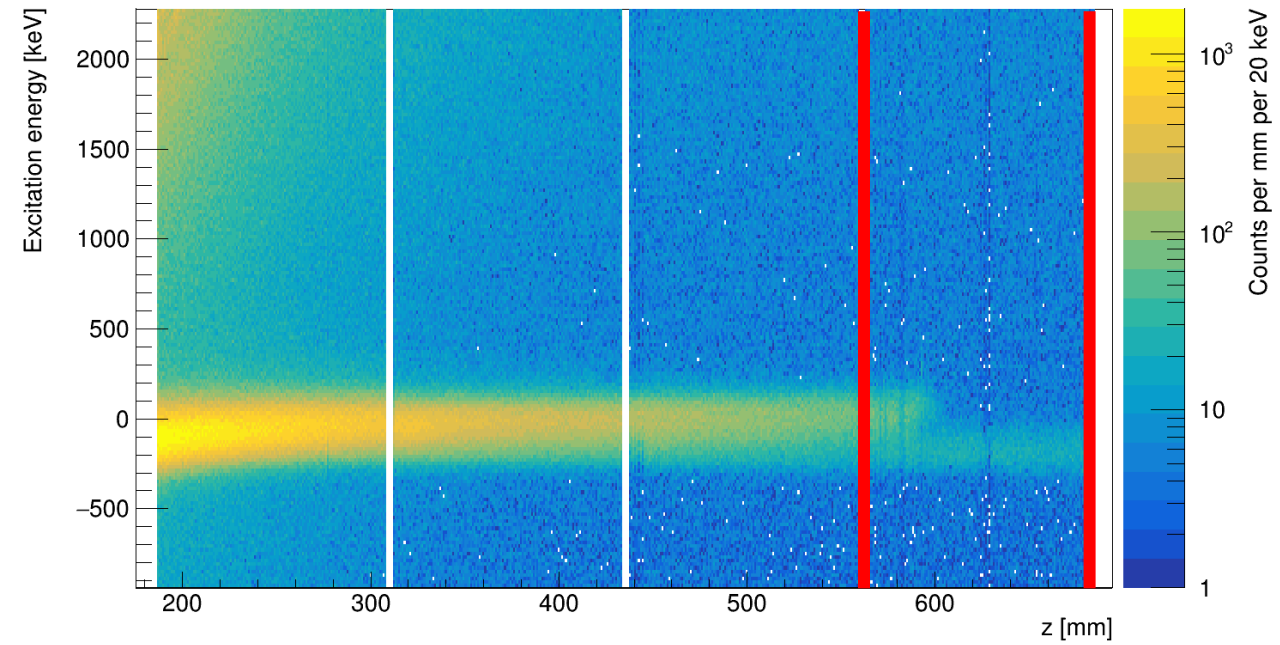
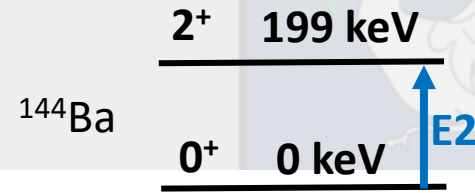


# ISS data



Excitation energy reconstructed from the kinematics

Slice of events from 570 mm to 684 mm

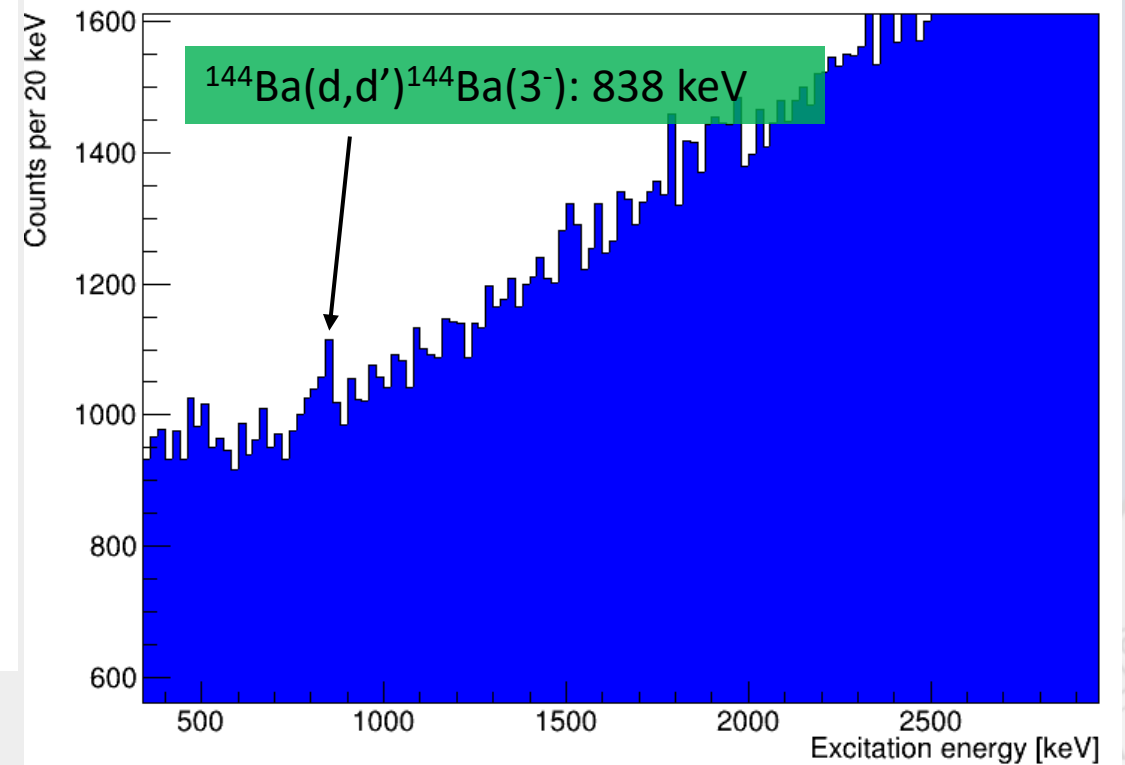
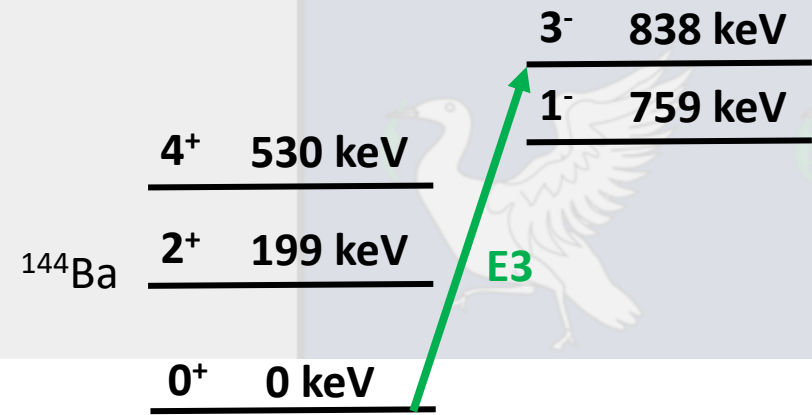
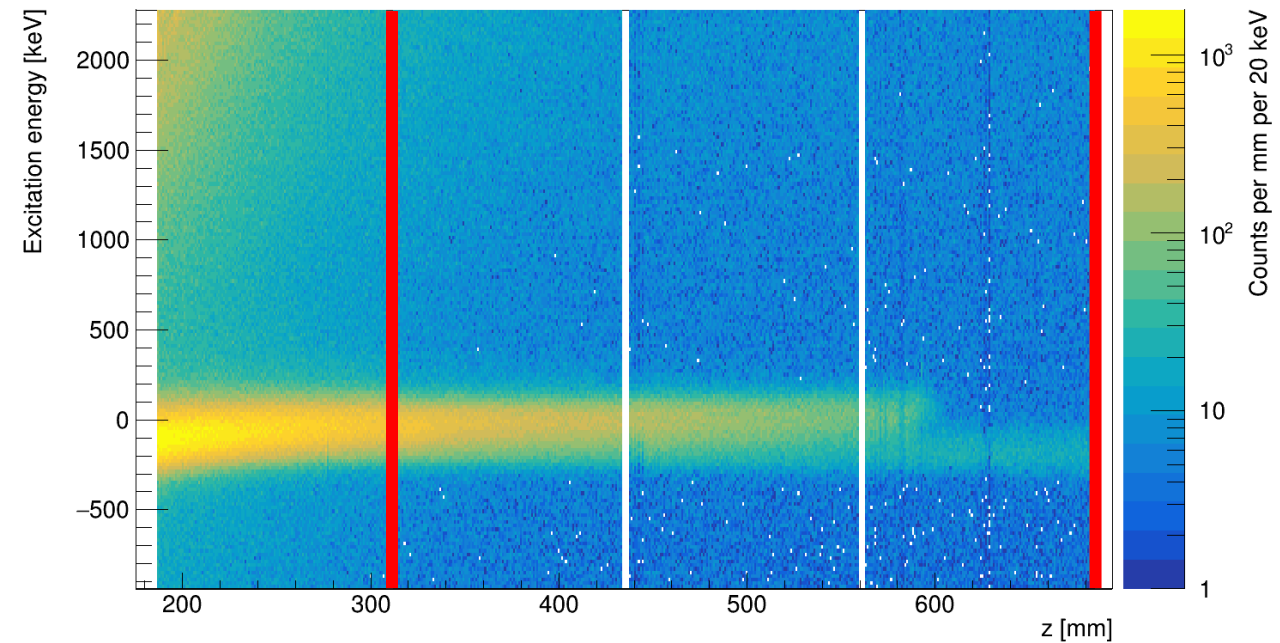


The  $2^+$  is only visible on the last row due to the resolution and size of the elastic peak.

Elastically scattered protons

Elastically scattered deuterons

Slice of events from 312 mm to 684 mm



Almost the entire detector can be used to see the  $3^-$  since its far enough away from the rutherford scattering peak.